Computer Assisted Mechanics and Engineering Sciences, 7: 717–734, 2000.

Approaches to enthalpy approximation in numerical simulation of two-component alloy solidification

Norbert Sczygiol
Technical University of Częstochowa, Institute of Mechanics and Machine Design
ul. Dąbrowskiego 73, 42–200 Częstochowa, Poland

(Received November 3, 1999)

The paper deals with the numerical modelling of solidification of two–component metal alloys. The numerical model was worked out using the enthalpy formulation of solidification and the finite element method. The work concentrated on one enthalpy formulation, namely the basic enthalpy formulation [11]. The models of solid phase growth as well as implementation details are shown in the paper [8]. A comparison of the results of the numerical simulation of solidification was made for three approaches to enthalpy approximation as a function of temperature. The three approaches were called: complete, incomplete and linear. The results of simulation, for incomplete enthalpy approximation were almost identical to the results of complete approximation. The computing time for incomplete approximation was substantially lower than the computing time for complete approximation, and comparable to the computing time for linear approximation.

1. Introduction

The pass from the liquid to the solid state is a process composed of many physical phenomena: heat transfer, liquid metal movement, evolution of the latent heat of solidification, diffusion of solute and others. Other phenomena, which mainly influence the usability value of the casting and occur as a result of the phenomena mentioned above, also have major significance. The creation of the structure is the most important of them. The structure is important because it determines the usability values of sound castings and also influences the course of thermo–mechanic states in the solidifying and cooling castings. Insufficient strength of solidifying layers could lead to the occurrence of casting defects, which often disqualifies them.

The majority of alloys solidify over a range of temperatures. The temperature at the beginning of alloy solidification is called the liquidus temperature (T_L), while the temperature at the end of solidification is called the solidus temperature (T_S). If, for instance, eutectic transformation can proceed in the solidifying alloy then eutectic temperature (T_E) can be the temperature of the end of solidification. In this case, the last stage of solidification proceeds at a constant temperature. The conditions of carrying away heat from the casting determine the temperature of the end of alloy solidification, where the amount of solute is smaller than its maximal solubility in the solid phase. There is no sharp separation between liquid and solid phases in the solidifying metal alloys. These phases are separated from each other by a so–called "mushy zone" (solidification front) in which both liquid and solid phases appear at the same time. The width of the mushy zone depends on the chemical constitution of the solidifying alloy and on the velocity of solidification (solid phase growth). The dynamic of the mushy zone determines the structure of the solidifying metal.

The finite element method is the most commonly used approach in numerical modelling and in numerical simulation of solidification. The above method was also applied in this paper with special respect to its suitability in connection with enthalpy formulation of solidification. The basic

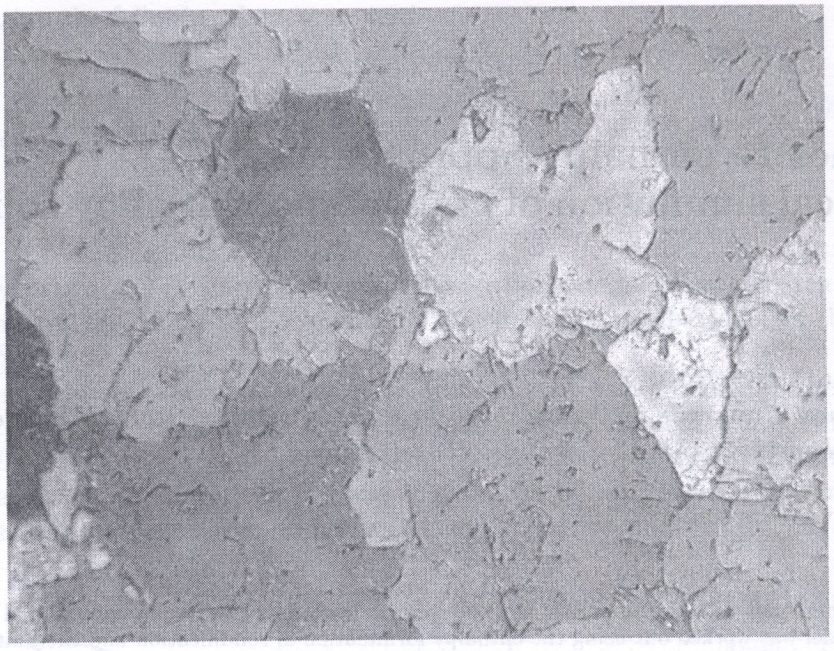

Fig. 1. Equiaxial grains in the Al–2%Cu alloy structure poured into metal form (50 × magnification)

enthalpy formulation directly takes into account the forming structure in the numerical model. This paper takes into consideration only the possibility of the formation of equiaxial structure (Fig. 1).

Many approaches to enthalpy approximation exist in the range of solidification temperatures [1, 3, 10, 12]. In the paper the solidification of two–component alloys was analysed and three approaches to enthalpy approximation were compared.

2. THE ENTHALPY FORMULATION OF SOLIDIFICATION

The solidification is stated by a quasi–linear heat conduction equation containing the term of heat source, which describes the rate of latent heat evolution

$$\nabla \cdot (\lambda \nabla T) + \rho_s L \frac{\partial f_s}{\partial t} = c\rho \frac{\partial T}{\partial t}\,, \tag{1}$$

where λ is the thermal conductivity coefficient, c is the specific heat, ρ is the density (subscript s refers to the solid phase, l refers to the liquid phase, f refers to the mushy zone), L is the latent heat of solidification and f_s is the solid phase fraction. This equation, together with suitable initial and boundary conditions, forms the basis of the thermal description of solidification.

Taking into consideration the enthalpy, defined as follows

$$H(T) = \int_{T_{\text{ref}}}^{T} c\rho(T)\,\mathrm{d}T + (1 - f_s(T))\,\rho_s L, \tag{2}$$

where T_{ref} is the reference temperature, and $c\rho$ is the heat capacity, one can pass to the class of enthalpy descriptions of solidification process. Differentiating the enthalpy, given by Eq. (2), with respect to time obtains the basic enthalpy formulation

$$\nabla \cdot (\lambda \nabla T) = \frac{\partial H}{\partial t}\,, \tag{3}$$

where

$$\frac{\partial H}{\partial t} = c\rho \frac{\partial T}{\partial t} - \rho_s L \frac{\partial f_s}{\partial t}\,. \tag{4}$$

First semi–discretisation (discretisation over space) of Eq. (3) and then time integration (discretisation over time) take place. The time integration is made by one of the one– or multi–step schemes [3, 12, 13]. Integration by a one–step scheme, for example the Euler backward scheme (EB), obtains a system of equations in which the coefficients of the left–hand side matrix are functions of the calculated temperatures. The application of these schemes makes it necessary to use iterative processes in every time step. The application of forward schemes, for example the Euler forward scheme (EF), often demands very small time steps to be used to reach a stable solution. This extends the calculation time. The calculation time can be shortened by applying two–step schemes, for example the Dupont II scheme [3], in which the coefficients of the left–hand side matrix are functions of extrapolated values of temperature, calculated on the basis of temperatures from the previous time steps. Two–step schemes require knowledge of enthalpy on two earlier time levels. That is why using a one–step scheme is indispensable in the first time step. In this paper the EB scheme was applied in the first time step and Dupont II in the remaining time steps. To avoid the iteration process in the first time step the so–called modified EB scheme (mEB) [13] was used. In the mEB scheme coefficients of the left–hand side matrix are functions of known values of temperature (in this case given by the initial conditions).

For the modified Euler backward scheme Eq. (3) takes the form [9]

$$\mathbf{M}\mathbf{H}^{n+1} + \Delta t\,\mathbf{K}^n\mathbf{T}^{n+1} = \mathbf{M}\mathbf{H}^n + \Delta t\,\mathbf{b}^{n+1}, \tag{5}$$

and for the Dupont II scheme

$$\mathbf{M}\mathbf{H}^{n+2} + \frac{3}{4}\Delta t\,\mathbf{K}^0\mathbf{T}^{n+2} = \mathbf{M}\mathbf{H}^n - \frac{1}{4}\Delta t\,\mathbf{K}^0\mathbf{T}^n + \frac{3}{4}\Delta t\,\mathbf{b}^{n+2} + \frac{1}{4}\Delta t\,\mathbf{b}^n, \tag{6}$$

while

$$\mathbf{M} = \int_{\Omega^e} \mathbf{N}^T\mathbf{N}\,\mathrm{d}\Omega, \tag{7}$$

$$\mathbf{K} = \int_{\Omega^e} \lambda\,\nabla^T\mathbf{N}\cdot\nabla\mathbf{N}\,\mathrm{d}\Omega, \tag{8}$$

$$\mathbf{b} = \int_{\Gamma} \mathbf{N}_\Gamma^T\mathbf{N}_\Gamma\,\mathrm{d}\Gamma\,\mathbf{q}, \tag{9}$$

where $\mathbf{M}$ is the mass matrix, $\mathbf{K}$ is the conductivity matrix, $\mathbf{H}$ is the enthalpy vector, $\mathbf{T}$ is the temperature vector and $\mathbf{b}$ is the vector of the nodal heat sources, whose values are calculated on the boundary conditions basis, $\mathbf{N}$ is the shape functions vector in Ω domain, $\mathbf{N}_\Gamma$ is the shape functions vector on Γ boundary and $\mathbf{q}$ is the vector of heat fluxes given at the boundary nodes. Superscript $(^0)$ denotes that material properties are calculated for extrapolated temperature

$$T = \frac{3}{2}T^{n+1} - \frac{1}{2}T^n. \tag{10}$$

Because enthalpies and temperatures are on the same time level on the left–hand side of Eqs. (5) and (6), the temperatures are expanded in the Taylor series. After substituting the two first terms of these expansions into Eqs. (5) and (6) one can obtain

– for mEB

$$\left(\mathbf{M} + \Delta t\,\mathbf{K}^n\left[\frac{\mathrm{d}\mathbf{T}}{\mathrm{d}\mathbf{H}}\right]^n\right)\mathbf{H}^{n+1} = \left(\mathbf{M} + \Delta t\,\mathbf{K}^n\left[\frac{\mathrm{d}\mathbf{T}}{\mathrm{d}\mathbf{H}}\right]^n\right)\mathbf{H}^n - \Delta t\,\mathbf{K}^n\mathbf{T}^n + \Delta t\,\mathbf{b}^{n+1}, \tag{11}$$

– for Dupont II

$$\left(\mathbf{M} + \frac{3}{4}\Delta t\,\mathbf{K}^0\left[\frac{\mathrm{d}\mathbf{T}}{\mathrm{d}\mathbf{H}}\right]^{n+1}\right)\mathbf{H}^{n+2} = \left(\mathbf{M} + \frac{3}{4}\Delta t\,\mathbf{K}^0\left[\frac{\mathrm{d}\mathbf{T}}{\mathrm{d}\mathbf{H}}\right]^{n+1}\right)\mathbf{H}^{n+1} - \frac{3}{4}\Delta t\,\mathbf{K}^0\mathbf{T}^{n+1} - \frac{1}{4}\Delta t\,\mathbf{K}^0\mathbf{T}^n + \frac{3}{4}\Delta t\,\mathbf{b}^{n+2} + \frac{1}{4}\Delta t\,\mathbf{b}^n. \tag{12}$$

The temperature derivative with respect to enthalpy is a diagonal matrix here.

3. THE APPROXIMATION OF ENTHALPY

By assuming that the latent heat of solidification can be evaluated in an arbitrary way, the enthalpy for an alloy which solidifies in the range of $(T_L - T_S)$ temperatures equals [3]

$$H = \begin{cases} \displaystyle\int_{T_{\text{ref}}}^{T} c\rho_s \, \mathrm{d}T & \text{for} \quad T < T_S \,, \\ \displaystyle\int_{T_{\text{ref}}}^{T_S} c\rho_s \, \mathrm{d}T + \int_{T_S}^{T} \left(c\rho_f - \rho_s L \frac{\mathrm{d}f_s}{\mathrm{d}T} \right) \mathrm{d}T & \text{for} \quad T_S \le T \le T_L \,, \\ \displaystyle\int_{T_{\text{ref}}}^{T_S} c\rho_s \, \mathrm{d}T + \rho_s L + \int_{T_S}^{T_L} c\rho_f \, \mathrm{d}T + \int_{T_L}^{T} c\rho_l \, \mathrm{d}T & \text{for} \quad T > T_L \,. \end{cases} \tag{13}$$

Knowledge of the relationship between heat capacity and temperature in the solidification temperatures range as well as knowledge of the solid phase fraction derivative with respect to temperature is needed to determine the alloy enthalpy above the temperature of the end of solidification. The analytical functions of the solid phase fraction with respect to temperature can be deduced from the solution of the solute diffusion equation for two–component alloys [5]. This method requires suitable simplifying assumptions for the chosen model of solid phase growth (equilibrium, non–equilibrium or indirect) [4, 6].

Assumption that heat capacity in the range of solidification temperatures is calculated in the same way as for the mixture of solid and liquid phases leads to

$$c\rho_f(T) = f_s(T)\, c\rho_s + (1 - f_s(T))\, c\rho_l \,, \tag{14}$$

where $c\rho_s = \text{const}$ and $c\rho_l = \text{const}$ and $c\rho_s \neq c\rho_l$. As a next step the functions describing the alloy enthalpy in that range for particular models of solid phase growth can be deduced. For the above assumptions concerning the heat capacity a linear dependency between enthalpy and temperature exists at temperatures lower than T_S (or T_E) and at temperatures higher than T_L.

In the equilibrium model of solid phase growth the following equation is valid

$$f_s(T) = \frac{1}{1-k} \frac{T_L - T}{T_M - T} \,, \tag{15}$$

where k is the solute partition coefficient[1]. Substituting this relationship into Eq. (14) and its derivative with respect to temperature into Eq. $(13)_2$ and making a suitable integration, obtains for the range of solidification temperatures

$$\begin{aligned} H(T) = {} & c\rho_s T_S + c\rho_l (T - T_S) + \frac{c\rho_l - c\rho_s}{1-k} \left((T_L - T_M) \ln \frac{T_M - T}{T_M - T_S} + T_S - T \right) \\ & + \rho_s L \frac{T_M - T_L}{1-k} \frac{T - T_S}{(T_M - T)(T_M - T_S)} \,. \end{aligned} \tag{16}$$

In the non–equilibrium model of solid phase growth the following equation is valid

$$f_s(T) = 1 - \left(\frac{T_M - T}{T_M - T_L} \right)^{\frac{1}{k-1}} \,. \tag{17}$$

[1]Equations for solid phase fraction in the solidifying two–component alloy were deduced assuming $k = \text{const}$

For this model of solid phase growth the enthalpy in the range of solidification temperatures is equal to

$$H(T) = c\rho_s T_E + c\rho_s(T - T_E) + \frac{k-1}{k}(c\rho_l - c\rho_s)(T_L - T_M)\left(\left(\frac{T_M - T}{T_M - T_L}\right)^{\frac{k}{k-1}} - \left(\frac{T_M - T_E}{T_M - T_L}\right)^{\frac{k}{k-1}}\right) + \rho_s L\left(\left(\frac{T_M - T}{T_M - T_L}\right)^{\frac{1}{k-1}} - \left(\frac{T_M - T_E}{T_M - T_L}\right)^{\frac{1}{k-1}}\right) + \rho_s L(1 - f_s^E), \tag{18}$$

where f_s^E is the solid phase fraction at the moment when eutectic temperature is reached, calculated according to Eq. (17).

In the indirect model of solid phase growth the following equation is valid [5]

$$f_s(T) = \frac{1}{1 - nk\alpha}\left(1 - \left(\frac{T_M - T}{T_M - T_L}\right)^{\frac{1-nk\alpha}{k-1}}\right), \tag{19}$$

where

$$\alpha = \frac{D_s t_f}{r_g^2}, \tag{20}$$

and D_s is the solute diffusion coefficient in the solid phase, t_f is the so–called local solidification time, r_g is the characteristic dimension of the grain and n is the coefficient describing the grain shape ($n = 2$ for plane grain (plate), $n = 4$ for cylindrical grain and $n = 6$ for spherical grain). The relationships for solid phase fractions for both the equilibrium solidification model (for $\alpha = 1/n$) and the non–equilibrium solidification model (for $\alpha = 0$) [5] can be deduced from Eq. (19). A certain $\Omega(\alpha)$ correction is applied in the numerical calculation instead of α coefficient because the direct use of α coefficient could lead inaccuracy in the results. For plane grains the above correction is equal to [2]

$$\Omega(\alpha) = \alpha\left(1 - \exp\left(-\frac{1}{\alpha}\right)\right) - \frac{1}{2}\exp\left(-\frac{1}{2}\alpha\right). \tag{21}$$

For the other shapes of grains it has yet to be determined.

Two cases for the determination of enthalpy are possible for the indirect model of solid phase growth. If the solidification ends at the eutectic temperature, which happens, when after replacing T_E into Eq. (19), the solid phase fraction is lower than 1, the enthalpy in the range of solidification temperatures equals

$$H(T) = c\rho_s T_E + c\rho_l(T - T_E) + \frac{c\rho_l - c\rho_s}{1 - nk\Omega}\left(T_E - T + (T_L - T_M)\frac{k-1}{k(1-n\Omega)}\left(\left(\frac{T_M - T}{T_M - T_L}\right)^{\frac{k(1-n\Omega)}{k-1}} - \left(\frac{T_M - T_E}{T_M - T_L}\right)^{\frac{k(1-n\Omega)}{k-1}}\right)\right) + \frac{\rho_s L}{1 - nk\Omega}\left(\left(\frac{T_M - T}{T_M - T_L}\right)^{\frac{1-nk\Omega}{k-1}} - \left(\frac{T_M - T_E}{T_M - T_L}\right)^{\frac{1-nk\Omega}{k-1}}\right) + \rho_s L(1 - f_s^E), \tag{22}$$

where f_s^E is calculated according to Eq. (19) in this case.

If, after substituting eutectic temperature into Eq. (19), the solid phase fraction is bigger than 1, then solidification ends in the $(T_S - T_E)$ temperature range. This temperature is equal to

$$T_{SE} = T_M - (T_M - T_L)(nk\Omega)^{\frac{k-1}{1-nk\Omega}}. \tag{23}$$

In this case the enthalpy in the range of solidification temperatures is equal to

$$H(T) = c\rho_s T_{SE} + c\rho_l (T - T_{SE}) + \frac{c\rho_l - c\rho_s}{1 - nk\Omega}\left(T_{SE} - T + (T_L - T_M)\frac{k-1}{k(1-n\Omega)}\left(\left(\frac{T_M - T}{T_M - T_L}\right)^{\frac{k(1-n\Omega)}{k-1}} - \left(\frac{T_M - T_{SE}}{T_M - T_L}\right)^{\frac{k(1-n\Omega)}{k-1}}\right)\right) + \frac{\rho_s L}{1 - nk\Omega}\left(\left(\frac{T_M - T}{T_M - T_L}\right)^{\frac{1-nk\Omega}{k-1}} - \left(\frac{T_M - T_{SE}}{T_M - T_L}\right)^{\frac{1-nk\Omega}{k-1}}\right). \tag{24}$$

The diagrams of enthalpy functions for Al–2%Cu alloy for the approach to enthalpy approximation shown above, i.e. the complete approximation, for all three models of solid phase growth, are shown in Fig. 2. The diagrams for the indirect model of solid phase growth have been made for $n = 2$ and $\alpha = 0.15$ (with the eutectic temperature being reached) and $n = 2$ and $\alpha = 2$ (without the eutectic temperature being reached).

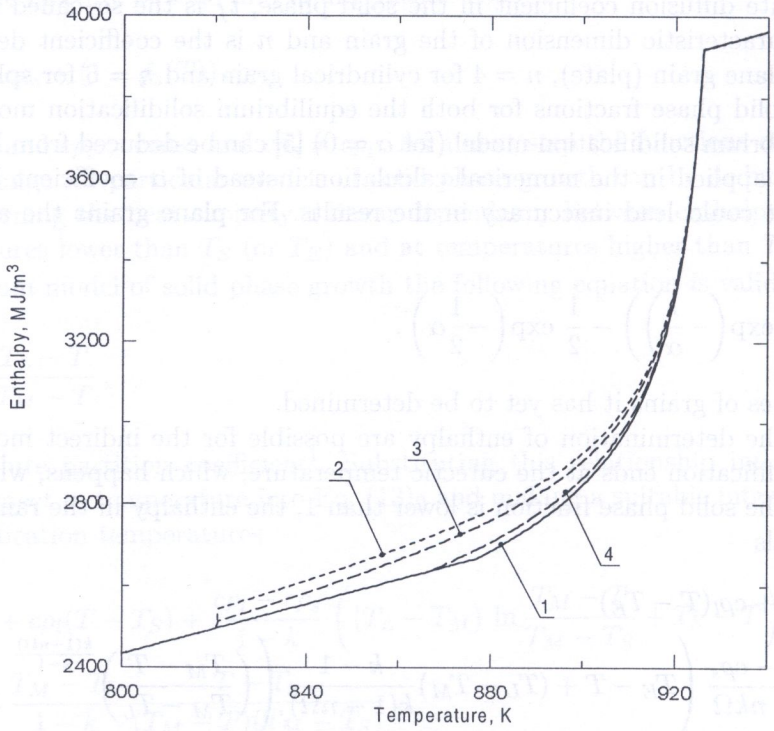

Fig. 2. Relationship of enthalpy to temperature in Al–2%Cu alloy for the complete approximation; 1 – equilibrium model, 2 – non-equilibrium model, 3 – indirect model with reaching T_E, 4 – indirect model without reaching T_E

The enthalpy equations, derived above, can be simplified by making the assumption that heat capacity in the range of solidification temperatures is the following arithmetic average,

$$c\rho_f = \frac{1}{2}(c\rho_s + c\rho_l). \tag{25}$$

Substituting this relationship into Eq. $(13)_2$ and carrying out suitable integration obtains

- for the equilibrium model of solid phase growth

$$H(T) = c\rho_s T_S + \frac{1}{2}(c\rho_s + c\rho_l)(T - T_S) + \rho_s L \frac{T_M - T_L}{1-k} \frac{T - T_S}{(T_M - T)(T_M - T_S)}, \tag{26}$$

- for the non–equilibrium model of solid phase growth

$$H(T) = c\rho_s T_E + \frac{1}{2}(c\rho_s + c\rho_l)(T - T_E) + \rho_s L \left(\left(\frac{T_M - T}{T_M - T_L} \right)^{\frac{1}{k-1}} - \left(\frac{T_M - T_E}{T_M - T_L} \right)^{\frac{1}{k-1}} \right) + \rho_s L \left(1 - f_s^E\right), \tag{27}$$

- for the indirect model of solid phase growth with T_E being reached

$$H(T) = c\rho_s T_E + \frac{1}{2}(c\rho_s + c\rho_l)(T - T_E) + \frac{\rho_s L}{1 - nk\Omega} \left(\left(\frac{T_M - T}{T_M - T_L} \right)^{\frac{1-nk\Omega}{k-1}} - \left(\frac{T_M - T_E}{T_M - T_L} \right)^{\frac{1-nk\Omega}{k-1}} \right) + \rho_s L \left(1 - f_s^E\right), \tag{28}$$

- for the indirect model of solid phase growth without T_E being reached

$$H(T) = c\rho_s T_{SE} + \frac{1}{2}(c\rho_s + c\rho_l)(T - T_{SE}) + \frac{\rho_s L}{1 - nk\Omega} \left(\left(\frac{T_M - T}{T_M - T_L} \right)^{\frac{1-nk\Omega}{k-1}} - \left(\frac{T_M - T_{SE}}{T_M - T_L} \right)^{\frac{1-nk\Omega}{k-1}} \right). \tag{29}$$

The diagrams of enthalpy functions for this approximation, i.e. incomplete approximation, for all three models of solid phase growth in Al–2%Cu alloy are shown in Fig. 3.

The simplest form of the relationship of enthalpy to temperature is obtained by calculating the enthalpy value at the temperature of the end of solidification and at the temperature of the beginning of solidification, assuming the linear dependence of enthalpy to temperature. These characteristic enthalpy values are as following

$$H = \begin{cases} c\rho_s T_S & \text{for} \quad T = T_S, \\ c\rho_s T_S + \rho_s L + \frac{1}{2}(c\rho_s + c\rho_l)(T_L - T_S) & \text{for} \quad T = T_L. \end{cases} \tag{30}$$

The enthalpy values at T_L temperature are the same for all models of solid phase growth. However, the enthalpy values for temperatures at the end of solidification are different. The enthalpy values at T_E temperature in the non–equilibrium model of solid phase growth are equal to

$$H = c\rho_s T_E + \rho_s L(1 - f_s^E), \tag{31}$$

where f_s^E value is calculated according to Eq. (17). The enthalpy value at T_E temperature is also calculated according to Eq. (31) in the indirect model of solid phase growth with the eutectic temperature being reached, but in this case the f_s^E value is calculated according to Eq. (19). The temperature at the end of solidification is calculated according to Eq. (23) in the indirect model of solid phase growth without the eutectic temperature being reached, while the enthalpy value at that temperature is evaluated according to Eq. $(30)_1$, in which T_S is replaced by T_{SE}. The diagrams of enthalpy functions for this approach to approximation, which will be called the linear approximation, are shown in Fig. 4.

The last stage of solidification always proceeds at a constant (eutectic) temperature in the non-equilibrium model of solid phase growth. In the indirect model of solid phase growth the solidification can also end at a constant temperature. With the above equations it is not possible to calculate the solid phase fraction at a constant temperature of solidification. The solid phase fraction is calculated assuming its linear dependency, from f_s^E to 1, in relation to temperature [9].

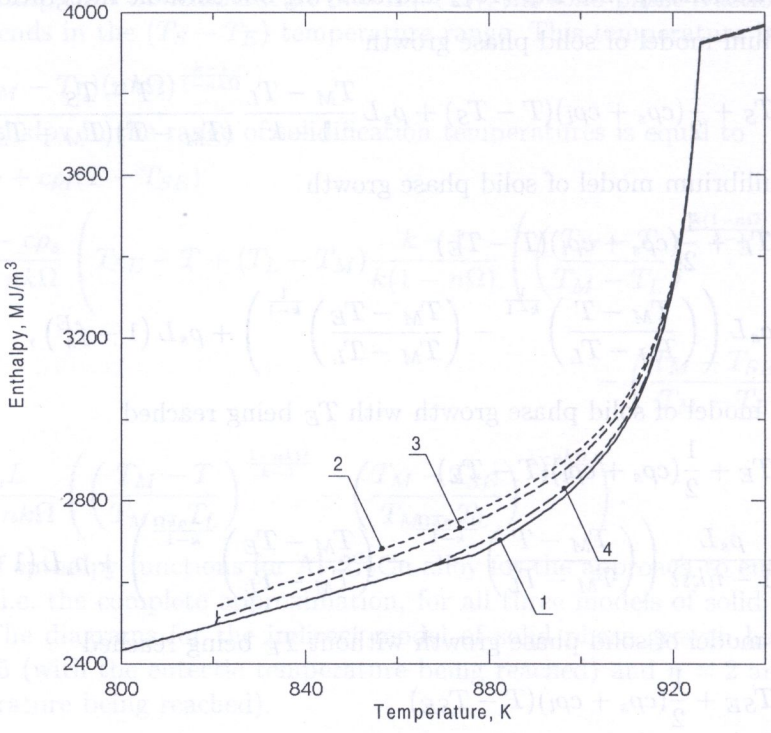

Fig. 3. Relationship of enthalpy to temperature in Al–2%Cu alloy for the incomplete approximation; 1 – equilibrium model, 2 – non–equilibrium model, 3 – indirect model with reaching T_E , 4 – indirect model without reaching T_E

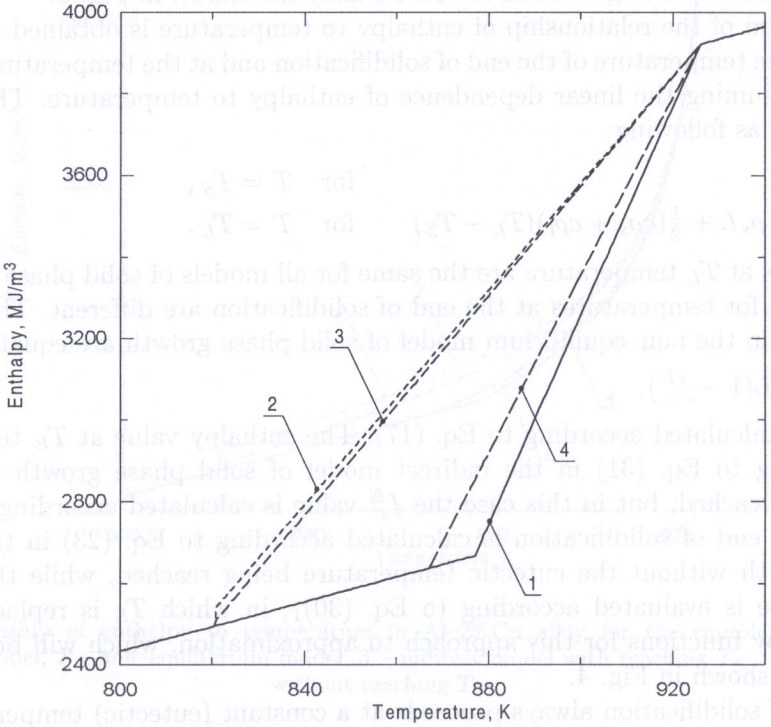

Fig. 4. Relationship of enthalpy to temperature in Al–2%Cu alloy for the linear approximation; 1 – equilibrium model, 2 – non–equilibrium model, 3 – indirect model with reaching T_E , 4 – indirect model without reaching T_E

4. Numerical model

Equations (11) and (12) are used to assemble the system of equations in the consecutive time step of the simulation. Equation (11) is completed with initial conditions, and both equations are completed with suitable boundary conditions, the numerical realisation of which is presented in paper [9]. Iterative methods are applied to solve the systems of equations because very often they are very large. Enthalpies are obtained from the solution of these systems of equations. Next, these enthalpies are recalculated on temperatures using one of the approaches to enthalpy approximation shown above. Temperature, obtained in this way, serves for an analysis of the solidification process. In dependency on the assumed model the solid phase fraction is calculated based on Eq. (15), (17) or (19). In the case of the indirect model of solid phase growth when the liquid metal reaches T_L temperature, the calculations are made with the aim of identifying if the solidification ends at T_E or a higher temperature. The grain size determines this.

The coefficients of the $\mathrm{d}\mathbf{T}/\mathrm{d}\mathbf{H}$ diagonal matrix from Eqs. (11) and (12) are calculated by differentiating Eq. (13) with respect to temperature. After a few transformations the following can be obtained

$$\frac{\mathrm{d}T}{\mathrm{d}H} = \begin{cases} 1/(c\rho_s) & \text{for} \quad T < T_S\,, \\ 1/\left(c\rho_f - \rho_s L \dfrac{\mathrm{d}f_s}{\mathrm{d}T}\right) & \text{for} \quad T_S \le T \le T_L\,, \\ 1/(c\rho_l) & \text{for} \quad T > T_L\,. \end{cases} \tag{32}$$

In the numerical model it was assumed that only equiaxial structure is formed in the casting. It was also assumed that the final grain radius is the characteristic dimension of this structure. The final grain radius depends on the average cooling velocity, i.e.

$$r_g = 0.14 + \ln(\dot{T})^{-0.0315}, \tag{33}$$

where $\dot{T}$ is the cooling velocity at the moment when the liquidus temperature is reached. This formula was obtained experimentally [9].

5. The examples of computer simulations

The computer simulations were carried out for an Al–2%Cu alloy which solidified in a metal mould. This alloy was chosen because of its wide range of solidification temperatures (49 K). The values of material properties, used in the calculations, were taken from paper [1]. For the liquid phase of the alloy: density 2498 kg/m^3, specific heat 1275 J/kgK and thermal conductivity coefficient 104 W/mK, while for the solid phase they are 2824 kg/m^3, 1077 J/kgK and 262 W/mK, respectively. The solidification heat of the alloy is equal to 390 kJ/kg and the solute partition coefficient equals 0.125. The material properties for the mould are: density 7500 kg/m^3, specific heat 620 J/kgK and thermal conductivity coefficient 40 W/mK. Temperatures were taken from a phase diagram for the Al–Cu alloy system. They are equal to: $T_M = 933$ K, $T_L = 926$ K, $T_S = 877$ K and $T_E = 821$ K. The initial temperature of the liquid alloy was 960 K, while the temperature of the mould was 660 K. The analysed casting together with the mould is shown in Fig. 5. The region is divided into 8609 triangular finite elements, obtaining 4659 nodes. The fourth type boundary condition with non–ideal contact was assumed between the casting and the mould (the conductivity of the separating layer was assumed to be equal to 1000 W/m^2 K). The third type boundary conditions were assumed on remaining boundaries. It was assumed that ambient temperature equals 300 K and heat exchange coefficient equals 100 W/m^{2}K on the top and the side boundaries, and 50 W/m^{2}K on the bottom boundary. A time step equal to 0.05 s was used in the calculations.

The computer simulations were carried out only for the indirect model of solid phase growth. This model was chosen because it allows calculated grain sizes in the successive calculations of solidification to be take into account (compare Eqs. (19) and (20)). In the evaluations of the α

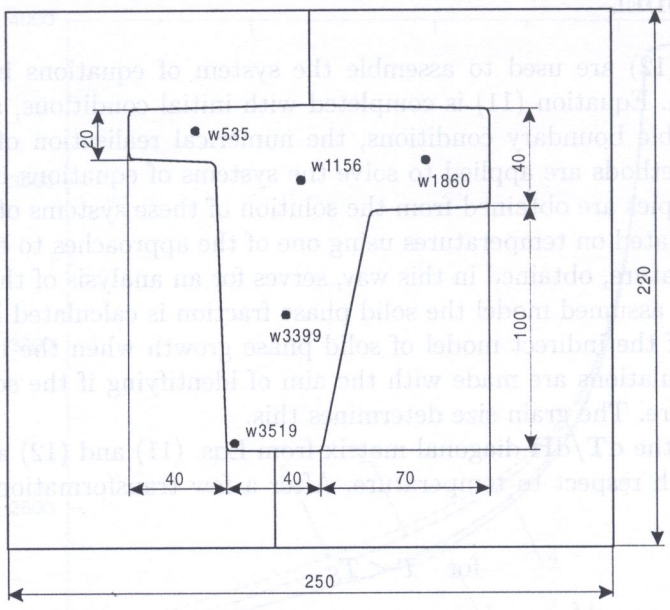

Fig. 5. The analysed casting in the mould

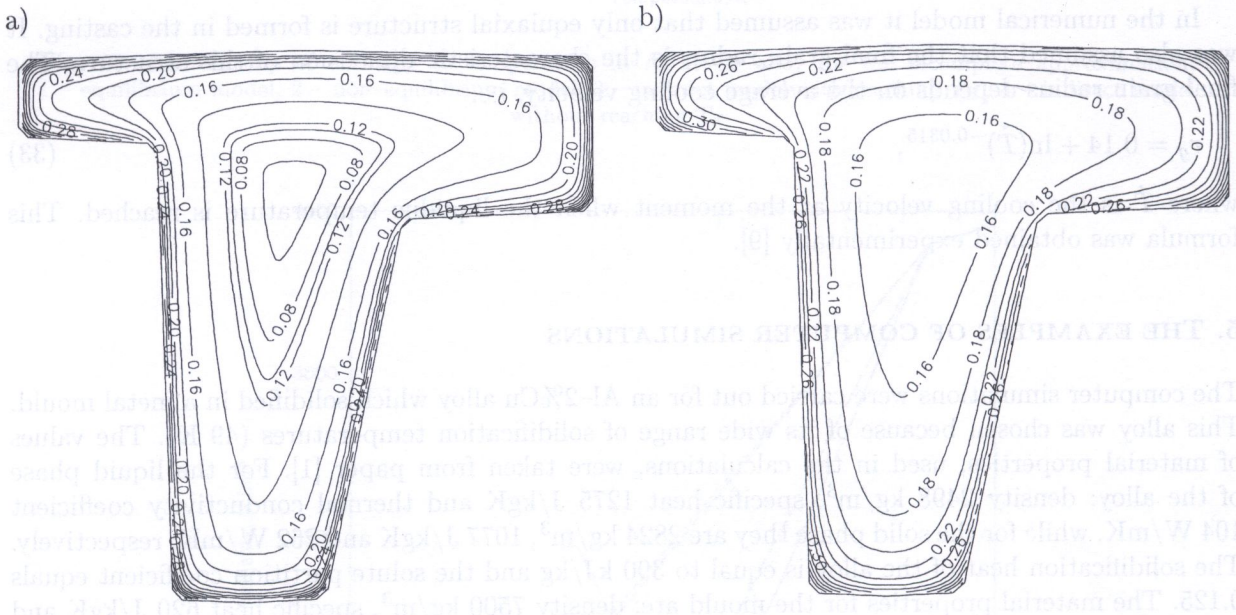

Fig. 6. The distribution of Ω parameter (see Eq. (21)); a) complete approximation, b) linear approximation

coefficient, it was assumed that $D_s t_f$ product equals $6 \cdot 10^{-9}$ m^2, while the coefficient of grain shape equals 2.

In the indirect model of solid phase growth the temperature at the end of solidification can change in the range from the equilibrium solidus temperature to the eutectic temperature. The Ω parameter is most important in the indirect model. It characterises the solidification of the alloy and can change from 0 to 0.5. In this interval there is a limit value, equal to 0.1988 for the alloy analysed here, below which the last portion of the liquid alloy solidifies at eutectic temperature. The distribution of Ω parameter in the casting is shown in Fig. 6. Only results for complete and linear approximation are shown in Figs. 6 to 10, because differences between results obtained for complete and incomplete enthalpy approximation are insignificantly small. Substantial differences of Ω parameter values occur

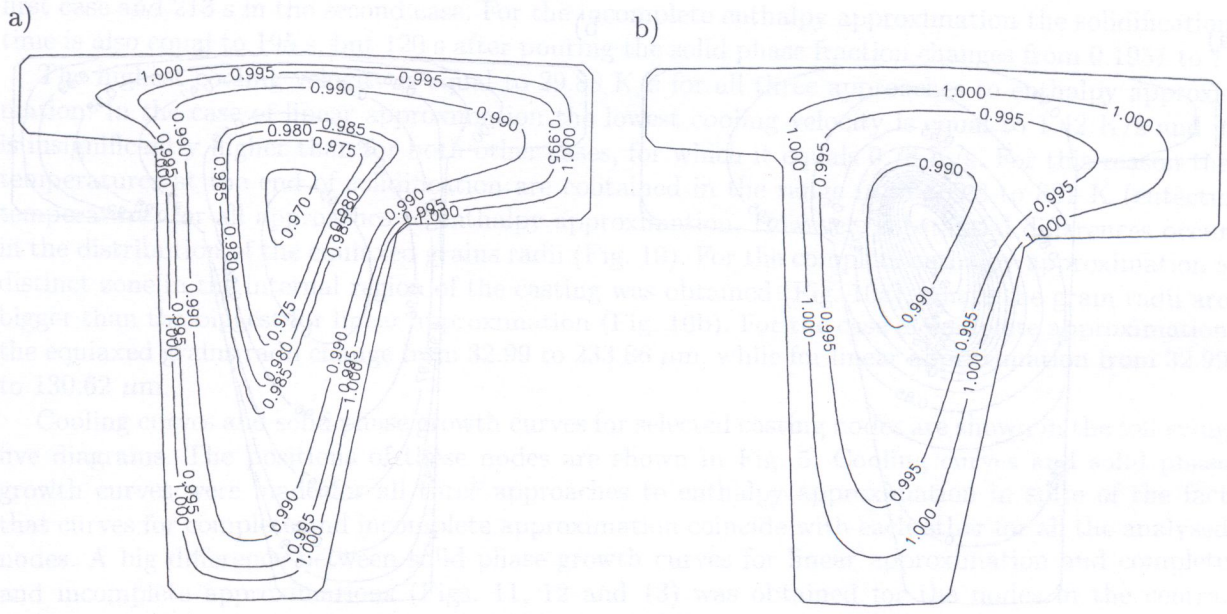

Fig. 7. The solid phase fraction distribution at the moment when the eutectic temperature was reached; a) complete approximation, b) linear approximation

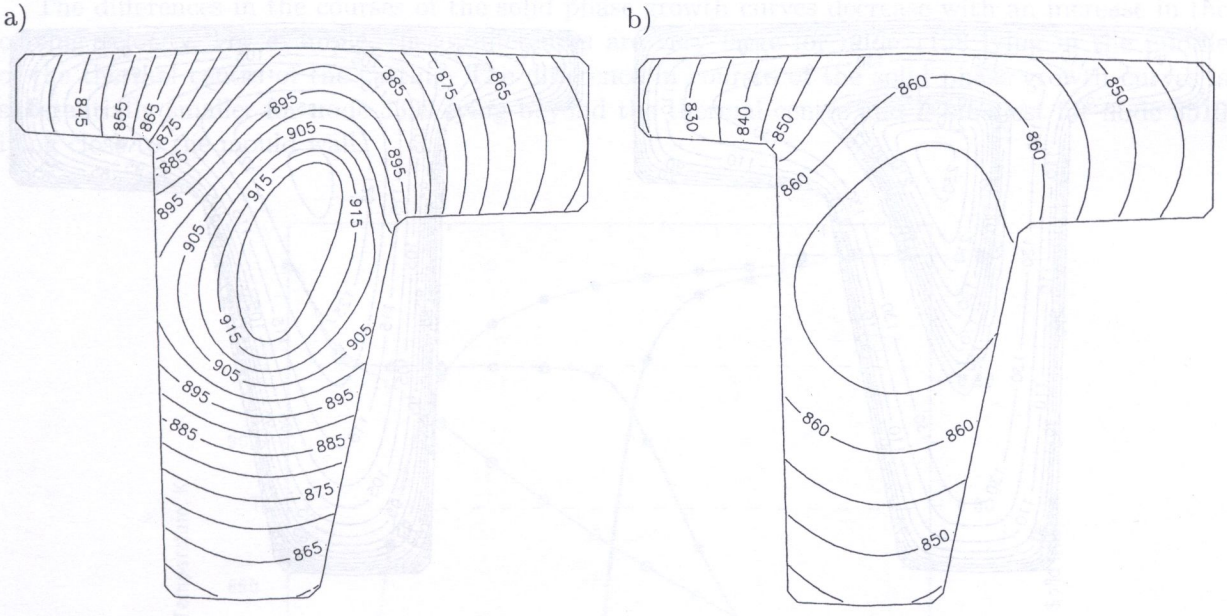

Fig. 8. The temperature field 120 s after pouring, K; a) complete approximation, b) linear approximation

in the middle zone of the casting, where the solidification ends at the eutectic temperature. The value of Ω parameter changes from 0.0548 to 0.4216 for the complete approximation (Fig. 6a), while for linear approximation it changes from 0.1461 to 0.4216 (Fig. 6b). The top values of both approaches to enthalpy approximation are the same because they were received for the regions being in contact with the mould wall, solidifying with the same velocity in both cases. The distributions of the solid phase fraction at the moment when the eutectic temperature is reached are shown in Fig. 7. The region where solidification ends at the eutectic temperature is much larger for the complete enthalpy approximation. Moreover, the amount of eutectic in this case (Fig. 7a) is significantly larger than for the linear enthalpy approximation (Fig. 7b).

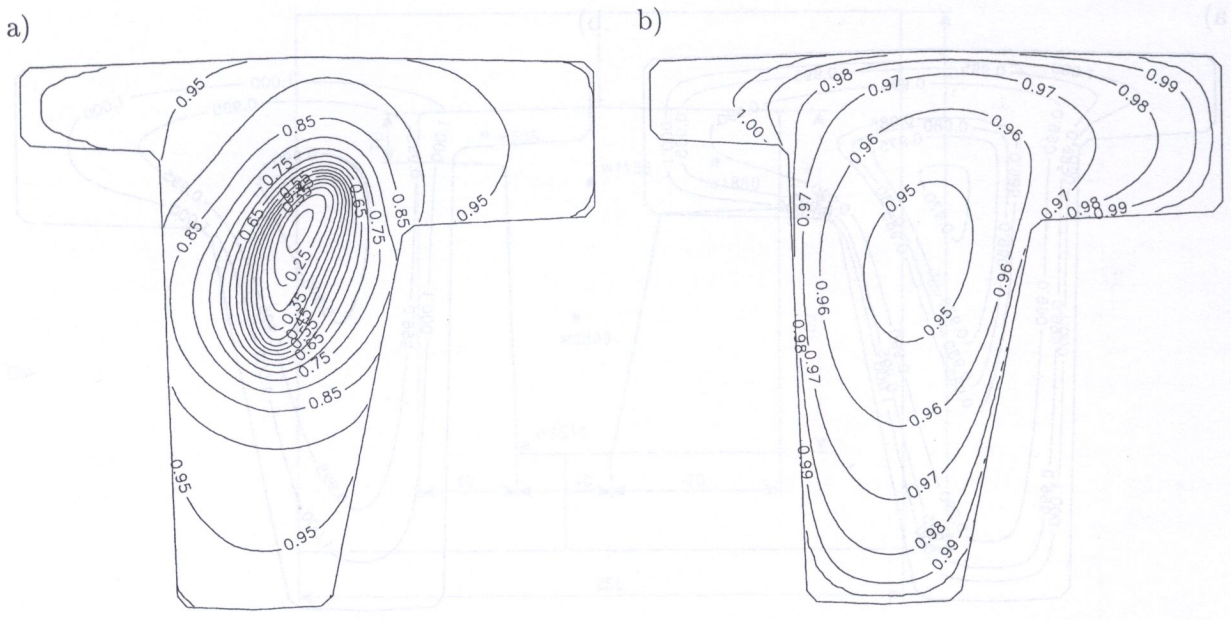

Fig. 9. The solid phase distribution 120 s after pouring; a) complete approximation, b) linear approximation

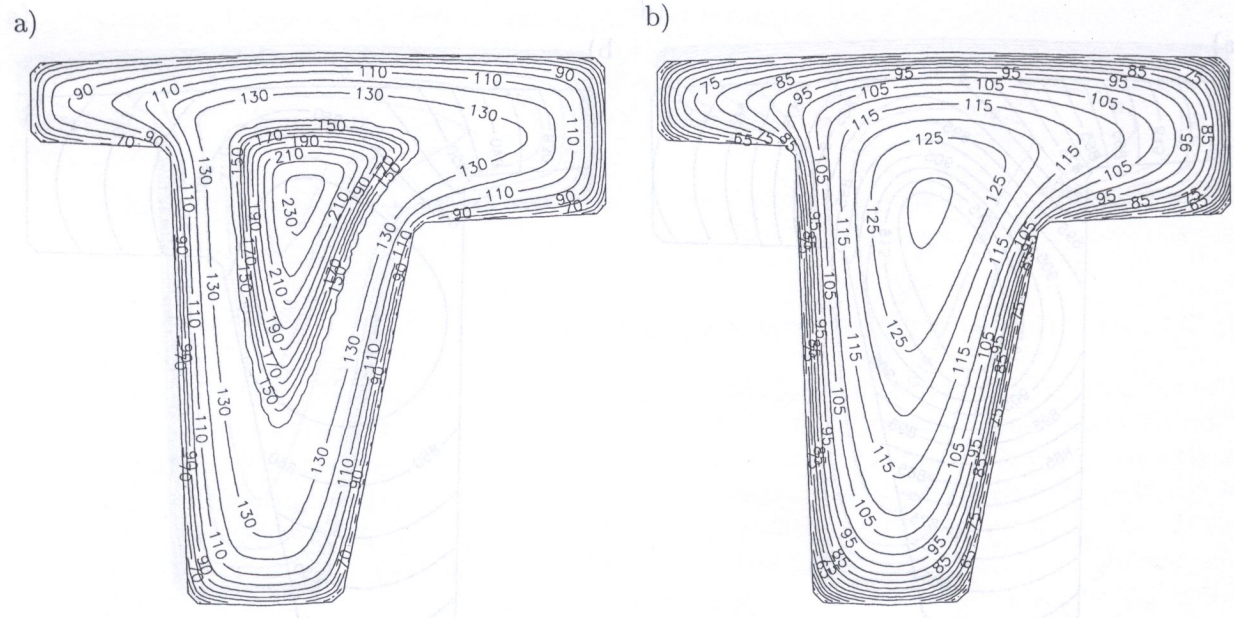

Fig. 10. The calculated average radii distribution, μm; a) complete approximation, b) linear approximation

The influence of the approach to enthalpy approximation on the temperature field is shown in Fig. 8. 120 s after pouring, noticeable differences in the temperature distributions occur. The lowest temperature for the complete enthalpy approximation equals 835.3 K, while the highest 924.6 K (Fig. 8a). For the linear approximation these temperatures are equal to 823.8 and 869.8 K, respectively.

At the initial stage of the casting solidification the solid phase growth is much slower for the complete enthalpy approximation (Fig. 9a). 120 s after pouring, the solid phase fraction changes in the range from 0.1831 to 1. For linear approximation the solid phase fraction is in the range from 0.9463 to 1 (Fig. 9b). In spite of this, the solidification time for the whole casting is shorter for the complete enthalpy approximation than for the linear approximation. It is equal to 195 s in the

first case and 213 s in the second case. For the incomplete enthalpy approximation the solidification time is also equal to 195 s, but 120 s after pouring the solid phase fraction changes from 0.1951 to 1.

The highest cooling velocity is equal to 29.88 K/s for all three approaches to enthalpy approximation. In the case of linear approximation the lowest cooling velocity is equal to 1.42 K/s and it is insignificantly higher than for both other cases, for which it equals 0.78 K/s. For this reason the temperatures at the end of solidification are contained in the range from 869.8 to 821 K (eutectic temperature) for all approaches to enthalpy approximation. However, substantial differences occur in the distribution of the equiaxed grains radii (Fig. 10). For the complete enthalpy approximation a distinct zone in the internal region of the casting was obtained (Fig. 10a), where the grain radii are bigger than the biggest for linear approximation (Fig. 10b). For the case of complete approximation the equiaxed grains radii change from 32.99 to 233.86 μm, while for linear approximation from 32.99 to 130.62 μm.

Cooling curves and solid phase growth curves for selected casting nodes are shown in the following five diagrams. The positions of these nodes are shown in Fig. 5. Cooling curves and solid phase growth curves were made for all three approaches to enthalpy approximation in spite of the fact that curves for complete and incomplete approximation coincide with each other for all the analysed nodes. A big difference between solid phase growth curves for linear approximation and complete and incomplete approximations (Figs. 11, 12 and 13) was obtained for the nodes in the central casting region (nodes 1156, 1860 and 3399). A big difference in the course of cooling curves also occurred for these nodes with distinct relatively long stops in the liquidus temperature for complete and incomplete approximations. This stop is considerably shorter for node 535 (Fig. 14) and it disappears completely in node 3519 (Fig. 15) which lies close to the mould wall.

The differences in the courses of the solid phase growth curves decrease with an increase in the cooling velocity. For example, these differences are very large for node 1158 lying in the middle of the thermal centre of the casting. The difference in courses of the solid phase growth curves is substantially smaller for node 3399 lying beyond the thermal centre and is smallest for node 3519 lying close to the mould wall.

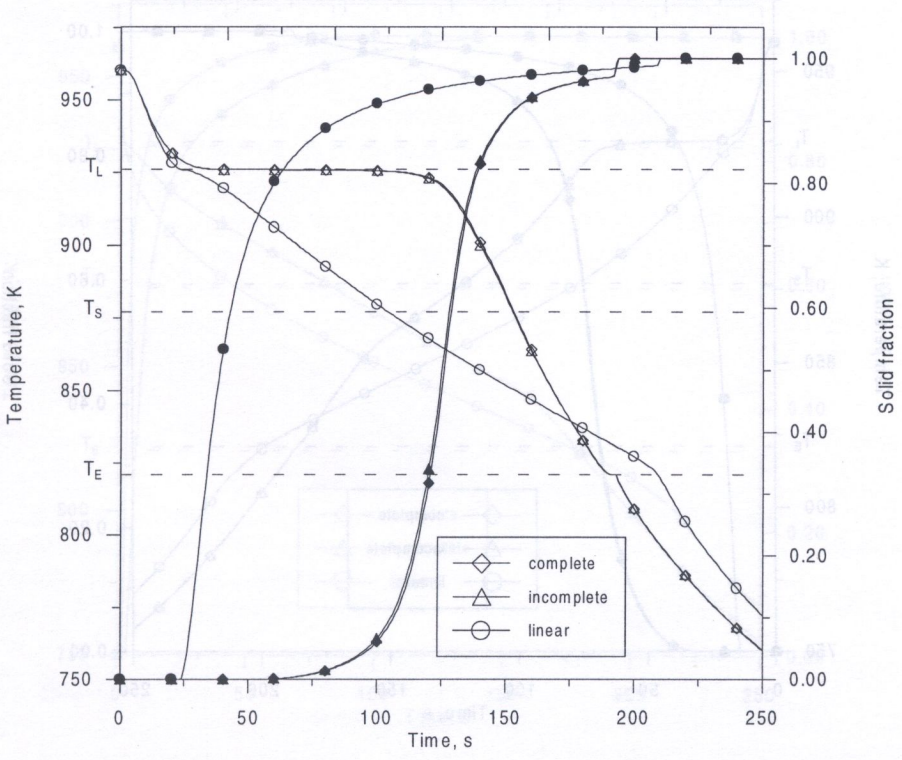

Fig. 11. Cooling curves and solid phase growth curves for the node 1156

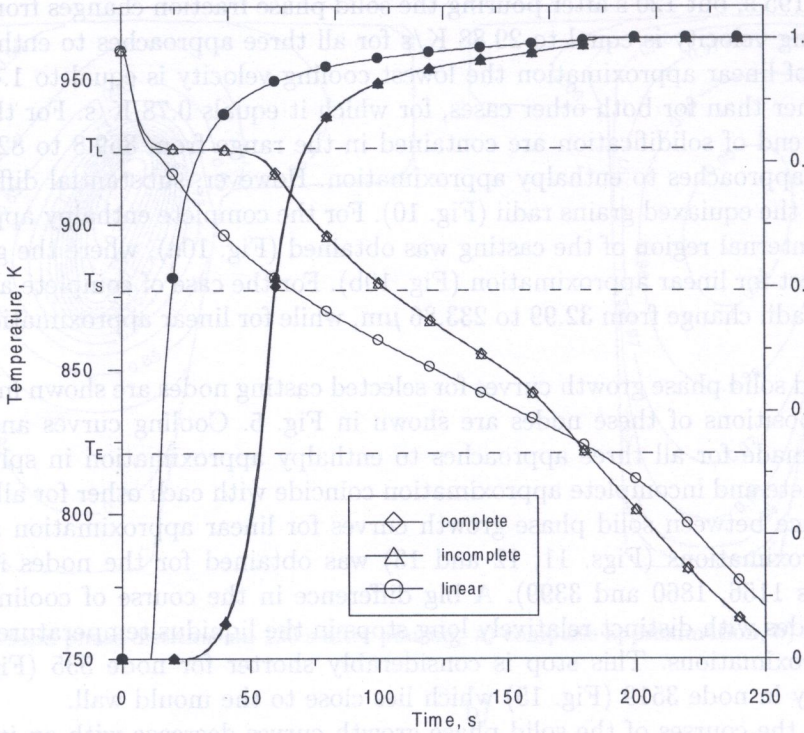

Fig. 12. Cooling curves and solid phase growth curves for the node 1860

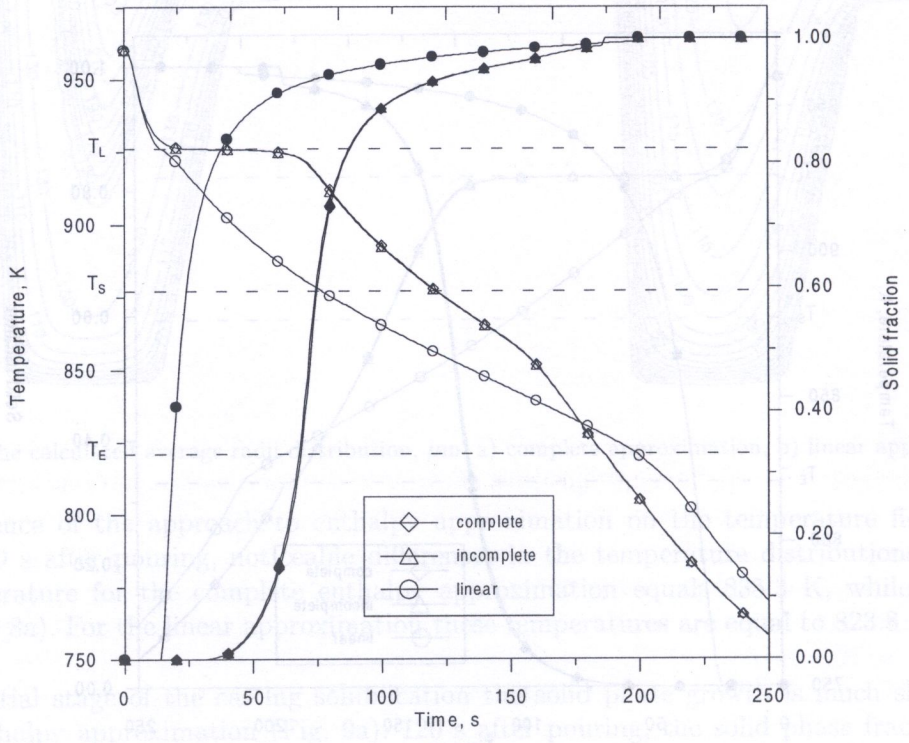

Fig. 13. Cooling curves and solid phase growth curves for the node 3399

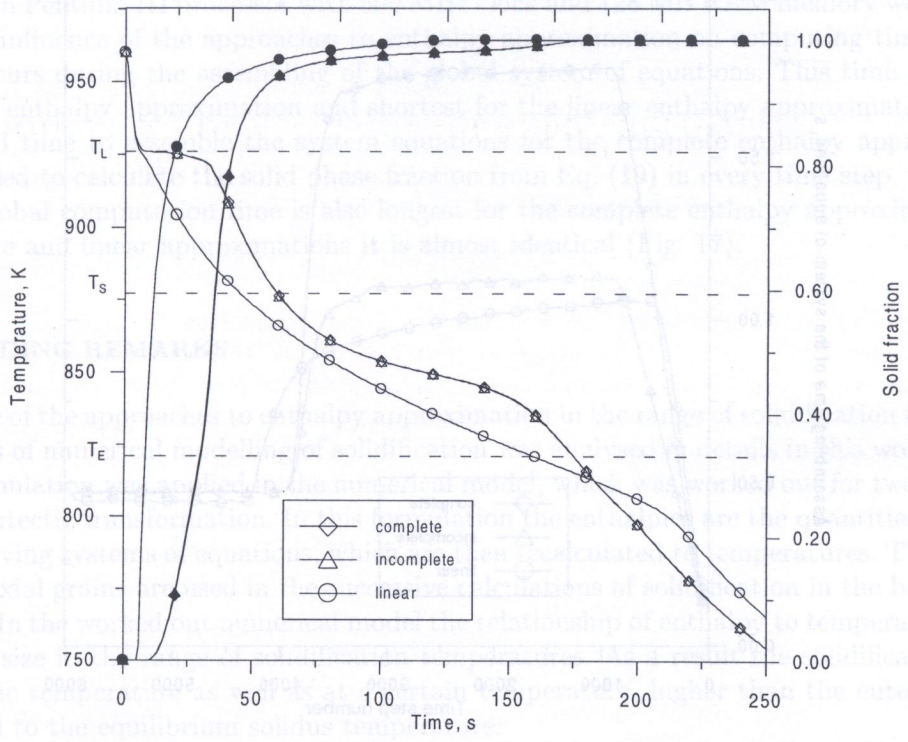

Fig. 14. Cooling curves and solid phase growth curves for the node 535

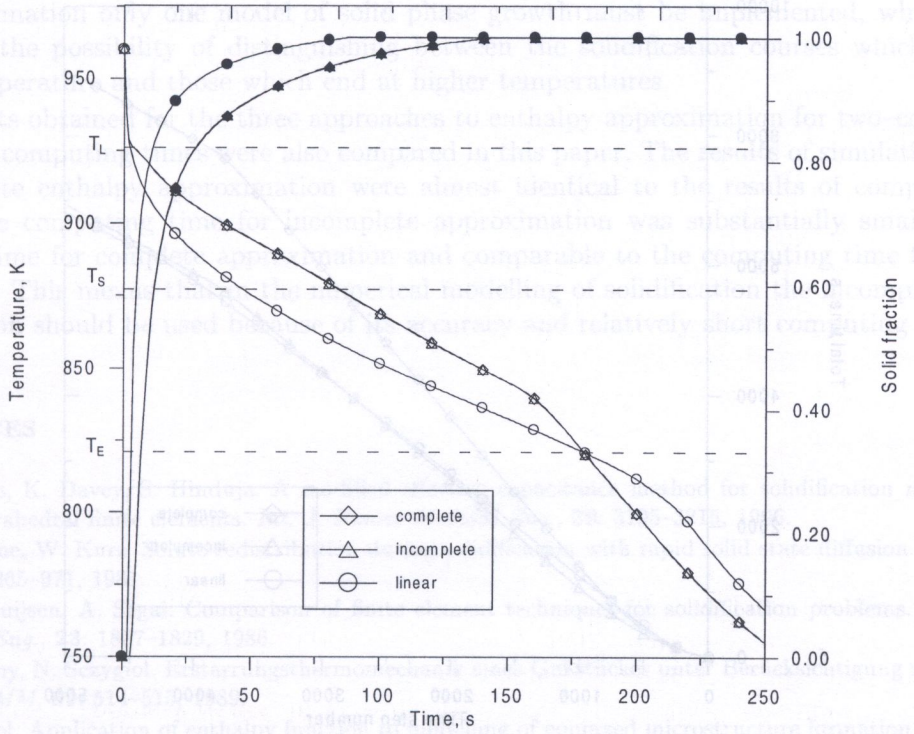

Fig. 15. Cooling curves and solid phase growth curves for the node 3519

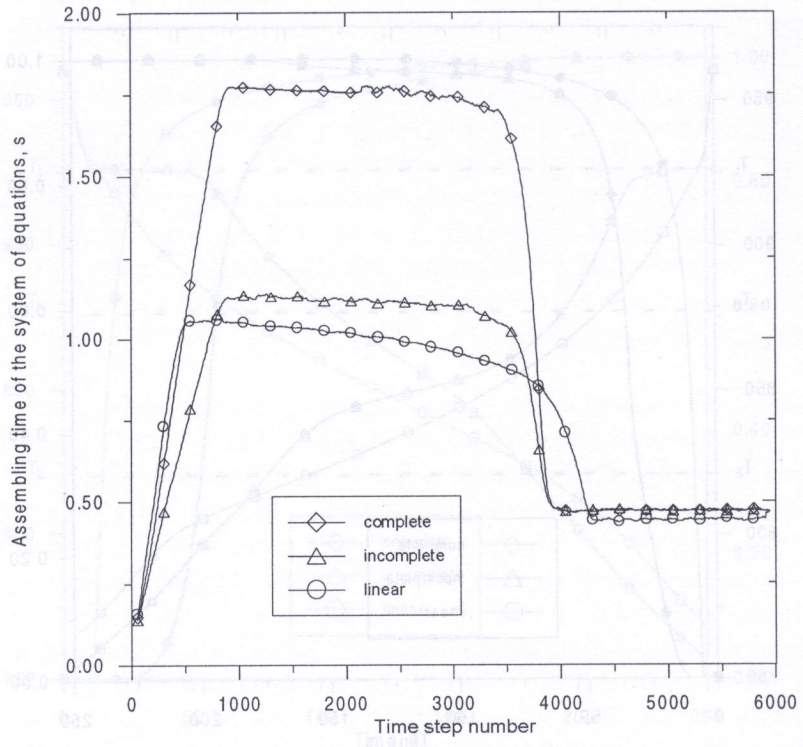

Fig. 16. The distribution of the assembling time of the systems of equations for particular approaches to enthalpy approximation

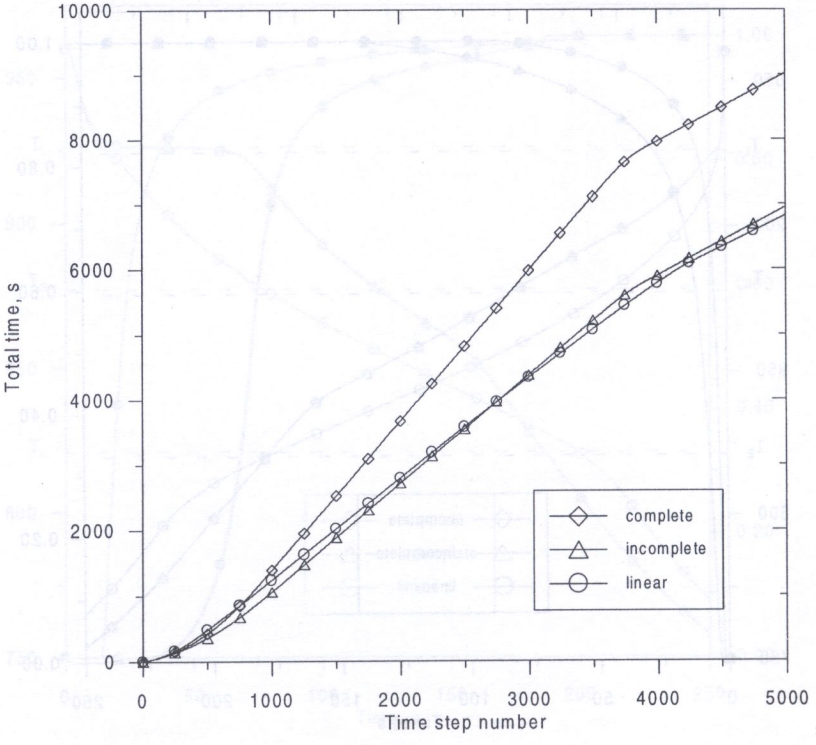

Fig. 17. The comparison of the total computing times for particular approaches to enthalpy approximation

The time taken to assemble the global system of equations and the global calculation time on a computer with Pentium III processor with 500 MHz clock and 128 MB RAM memory were compared to check the influence of the approaches to enthalpy approximation on computing time. The basic difference occurs during the assembling of the global system of equations. This time is longest for the complete enthalpy approximation and shortest for the linear enthalpy approximation (Fig. 16). The extended time to assemble the system equations for the complete enthalpy approximation is due to the need to calculate the solid phase fraction from Eq. (19) in every time step. For the same reason the global computation time is also longest for the complete enthalpy approximation, while for incomplete and linear approximations it is almost identical (Fig. 17).

6. Concluding remarks

The influence of the approaches to enthalpy approximation in the range of solidification temperatures on the results of numerical modelling of solidification was analysed in details in this work. The basic enthalpy formulation was applied in the numerical model, which was worked out for two–component alloys with eutectic transformation. In this formulation the enthalpies are the quantities obtained as a result of solving systems of equations, which are then recalculated to temperatures. The calculated radii of equiaxial grains are used in the successive calculations of solidification in the basic enthalpy formulation. In the worked out numerical model the relationship of enthalpy to temperature depends on the grain size in the range of solidification temperatures. As a result the solidification can end at the eutectic temperature as well as at a certain temperature, higher than the eutectic one, but at least equal to the equilibrium solidus temperature.

Three approaches to enthalpy approximation (complete, incomplete and linear) for three models of solid phase growth (equilibrium, non–equilibrium and indirect) were discussed. In all three cases the diagrams describing the relationships between the enthalpy and the temperature for equilibrium and non–equilibrium solid growth models can be obtained from the indirect model by using appropriate values of the Ω parameter. In this way, in numerical modelling of solidification and structure formation only one model of solid phase growth must be implemented, which of course should give the possibility of distinguishing between the solidification courses which end at the eutectic temperature and those which end at higher temperatures.

The results obtained for the three approaches to enthalpy approximation for two–component alloys and the computing times were also compared in this paper. The results of simulation, obtained for incomplete enthalpy approximation were almost identical to the results of complete approximation. The computing time for incomplete approximation was substantially smaller than the computing time for complete approximation and comparable to the computing time for linear approximation. This means that in the numerical modelling of solidification the incomplete enthalpy approximation should be used because of its accuracy and relatively short computing time.

References

[1] S. Bounds, K. Davey, S. Hinduja. A modified effective capacitance method for solidification modelling using linear tetrahedral finite elements. *Int. J. Numer Methods Eng.*, **39**: 3195–3215, 1996.

[2] T.W. Clyne, W. Kurz. Solute redistribution during solidification with rapid solid state diffusion. *Metall. Trans. A*, **12A**: 965–971, 1981.

[3] A.J. Dalhuijsen, A. Segal. Comparison of finite element techniques for solidification problems. *Int. J. Numer Methods Eng.*, **23**: 1807–1829, 1986.

[4] R. Parkitny, N. Sczygiol. Erstarrungsthermomechanik eines Gußstückes unter Berücksichtigung seines Kornaufbaus. *ZAMM*, **69**: 514–515, 1989.

[5] N. Sczygiol. Application of enthalpy function to modelling of equiaxed microstructure formation in castings. In: Ch. Hirsch *et al.* (eds.) *Numerical Methods in Engineering '92*, 205–208. Elsevier Science Publishers, 1992.

[6] N. Sczygiol. Das rechnerische Modellieren der Beimengungsverteilung in erstarrenden Gußstücken aus binären Legierungen. *ZAMM*, **74**: 619–622, 1994.

[7] N. Sczygiol. *Numerical Modelling of Thermo–Mechanical Phenomena in a Solidifying Casting and a Mould.* Technical University of Częstochowa Press, Częstochowa, 2000.

[8] N. Sczygiol. Object–oriented analysis of the numerical modelling of castings solidification. *Computer Assisted Mechanics and Engineering Sciences*, 2001 (in print).

[9] N. Sczygiol, G. Szwarc. Application of enthalpy formulations for numerical simulation of castings solidification. *Computer Assisted Mechanics and Engineering Sciences*, 2001 (in print).

[10] C.R. Swaminathan, V.R. Voller. A general enthalpy method for modeling solidification processes. *Metall. Trans. B*, **23B**: 651–664, 1992.

[11] Ph. Thevoz, J.L. Desbiolles, M. Rappaz. Modeling of equiaxed microstructure formation in casting. *Metall. Trans. A*, **20A**: 311–322, 1989.

[12] V.R. Voller, C.R. Swaminathan, B.G. Thomas. Fixed grid techniques for phase change problems: A review. *Int. J. Numer. Methods Eng.*, **30**: 875–898, 1990.

[13] W.L. Wood. *Practical Time–Stepping Schemes.* Clarendon Press, Oxford, 1990.